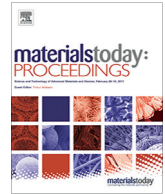




Contents lists available at ScienceDirect

Materials Today: Proceedings

journal homepage: www.elsevier.com/locate/matpr

Investigation on CFRP 3D printing build parameters and their effect on topologically optimised complex models

Arivazhagan Anbalagan^{a,b,1,*}, Edward James Launchbury^a, Marcos Kauffman^{a,b}, Ashwath Pazhani^a, Michael Anthony Xavier^c

^a Faculty of Engineering, Environment & Computing, Coventry University, Coventry CV1 5FB, UK

^b The Institute for Advanced Manufacturing & Engineering, (AME), Beresford Avenue, Coventry University, Coventry CV6 5LZ, UK

^c Vellore Institute of Technology, Vellore – 632014, Tamilnadu, India

ARTICLE INFO

Article history:
Available online xxx

Keywords:
Carbon Fibre Reinforcement (CFR)
Additive Manufacturing
Build parameters
Mechanical properties

ABSTRACT

This research investigates the effects of building parameters for 3D printing Carbon Fibre Reinforced Polymers (CFRP) and their effect on topologically optimised complex models. The work is conducted by initially developing a DOE varying two parameters in 3D printing namely (i) infill ratio and (ii) infill pattern. Then based on standards ASTM D638 and ISO178, for tensile and flexural tests, specimens are 3D printed and tested for the material Nylon with CFRP (Onyx). From the results it can be observed that (i) specimen with an infill ratio of 85% (constant triangular infill pattern) was found to have the best performance recording a length extension of approximately 5.6 mm under a tensile load of 700 N (ii) in case of infill pattern, triangular shape (constant infill ratio of 37%) recorded the highest the length extension of 7.3 mm under tensile load of 650 N. (iii) 85% infill ratio (constant triangular infill pattern) recorded a bending deflection of approximately 6 mm under a compressive load of 250 N and (iv) the gyroid infill pattern (constant infill ratio of 37%) provided the highest flexural strength with an approximate extension of 5.6 mm under a compressive load of 350 N. After the experimental study and analysing the best parameters, a static analysis and topology optimisation for the 3D printed material (Nylon with CFRP (Onyx)) has been performed on an industrial part for its design validation. Based on the analysis, the original part is redesigned, and again a static analysis simulation is performed to determine the effects of the optimisation process for the same material comparing with 316L-Stainless Steel (SS). Finally, the redesigned model is manufactured with the best 3D printing parameters and validated against the original operating conditions. This study will help industries to use these 3D printing parameters where a metal-based components needs to be replaced with CFRP.

Copyright © 2023 Elsevier Ltd. All rights reserved.

Selection and peer-review under responsibility of the scientific committee of the 16th Global Congress on Manufacturing and Management 2022. This is an open access article under the CC BY-NC-ND license (<http://creativecommons.org/licenses/by-nc-nd/4.0/>).

1. Introduction and literature review

In the recent years, advancements in 3D printing can be attributed to the increase in the use of product analysis, modelling and invention of new materials, optimisation of design and manufacturing capabilities through cloud computing and internet-based

* Corresponding author at: Assistant Professor (Research) in Digital Manufacturing, UK.

E-mail address: ad8181@coventry.ac.uk (A. Anbalagan).

¹ Dr. Arivazhagan Anbalagan is presently an Assistant Professor (Research) in Digital Manufacturing at The Institute for Advanced Manufacturing & Engineering, (AME), Coventry University. His research involves Digital Twin / Industry 4.0 / CAD / CAM / CAPP / CAE / CNC Machining / Manufacturing Technologies.

<https://doi.org/10.1016/j.matpr.2023.04.352>

2214-7853/Copyright © 2023 Elsevier Ltd. All rights reserved.

Selection and peer-review under responsibility of the scientific committee of the 16th Global Congress on Manufacturing and Management 2022.

This is an open access article under the CC BY-NC-ND license (<http://creativecommons.org/licenses/by-nc-nd/4.0/>).

Please cite this article as: A. Anbalagan, E.J. Launchbury, M. Kauffman et al., Investigation on CFRP 3D printing build parameters and their effect on topologically optimised complex models, Materials Today: Proceedings, <https://doi.org/10.1016/j.matpr.2023.04.352>

technologies. This current period of manufacturing development referred to as the 'Fourth Industrial Revolution' or 'Industry 4.0' makes 3D printing as one of the cores of its technological pillars. (Fig. 1(a)). Due to this, rigorous research in the last decade on 3D printing opened many new methods. Among them, one that is commonly used is Fused Filament Fabrication (FFF) also known as Fused Deposition Modelling (FDM) (Fig. 1(b)). Basically, it involves heating a nozzle [1] which then has the material filament pushed through and deposited to form the layers of the build. This process being the easy to adopt, several plastic materials are used in wired form and with metals / alloys added in the recent years [2]. Fig. 2(a) shows some examples of the materials used for 3D printing with some main advantages and disadvantages.

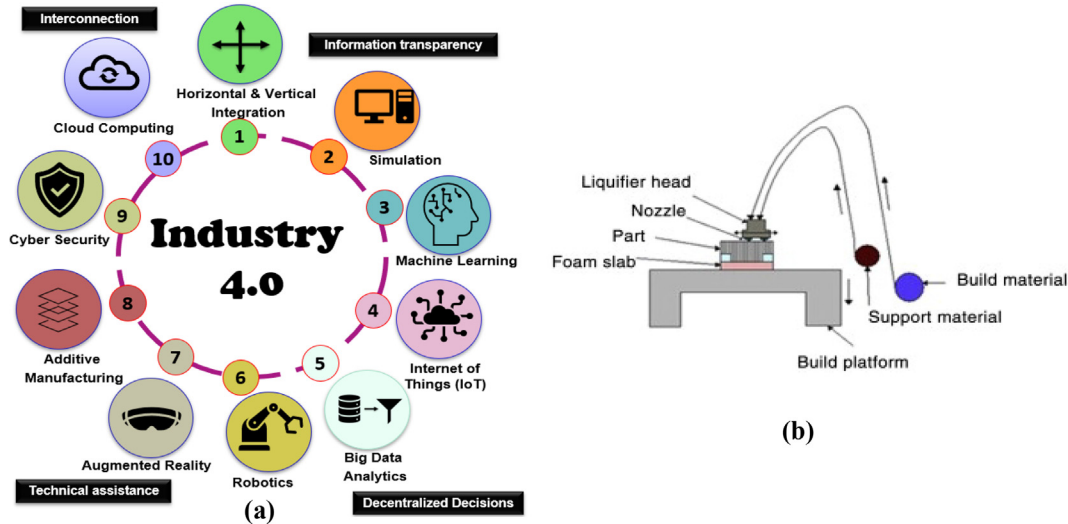
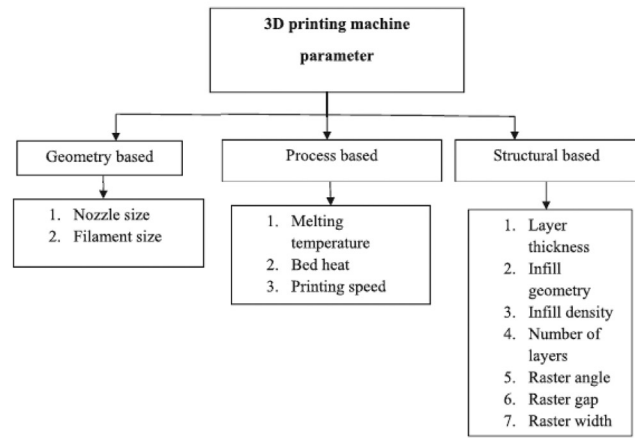


Fig. 1. (a) Core technologies forming 10 pillars of Industry 4.0 (b) Schematic diagram of Fused Deposition modelling [1].

Material	Advantage	Disadvantage
ABS	-Printability -Optimal cost -Good impact resistance -Low production time -Low electricity conductance	-Less chemical resistance -Weaker than other plastics -Non-eco-friendly
Nylon	-Flexibility -Durability -Toughness -Malleability	-High heating temperature -High bed temperature -Moist air absorption
CFRP	-High strength to weight ratio -Lightweight -Suitable aesthetics -Resistance to corrosion -Resistance to fatigue -Durability	-Expensive -Time-consuming manufacture -Not eco-friendly
Wood	-Eco-friendly material -Resistance to rust -Pleasure with the aesthetics -Satisfactory strength to weight ratio	-Lower elasticity modulus -Lower tensile strength -Variation of the mechanical properties
Metal	-High tensile strength -Modular design -Tear-resistance -High heat insulation	-Heavy -Bulky -Energy consuming production -Non-biodegradable -Extraction of chemical waste during production

(a)



(b)

Fig. 2. (a) Advantages and Disadvantages of Materials used in 3D Printing [2] (b) Build Parameters for 3D Printing [3].

In the FDM process, build parameters (Fig. 2 (b)) are the main features and many times altered to improve part performance, quality, cost, and print time [3]. With the recent rapid usage of carbon fibre in automobile, aerospace and oil & gas domains, there has been more attention on how these parameters affects the performance on a 3D printed CFRP. Ting Wang et.al. (2021) [4], analysed Voronoi diagram to find the effect of load dependent 3D printing speed for improving the mechanical properties of the Carbon Fibre Reinforced Polymers (CFRP). They achieved this by adopting a topology optimisation tool, then by developing a ‘Stress Vector Tracing’ algorithm.

Naoya Kumekawa et.al, (2021) [5], verified 3D printed CFRP’s by varying the thickness of the layer through modifying the height of the nozzle. Finite element software ANSYS Mechanical APDL (MAPDL) and MATLAB were used for optimizing fibre path and thickness. Keiichi Shirasu et.al. (2022) [6], analysed the bond strength for three-dimensional-printed titanium (3DP-Ti) adherends co-bonded with carbon fiber reinforced phenolic matrix composite (CFRP-MC). They used selective laser melting for 3DP-Ti and co-bonded with woven-fabric CFRP-MC by hot pressing. Jumpei Kajimoto et al. (2022) [7] analysed tensile strength through auto-

matically embedding carbon fiber reinforced polymer (CFRP) and epoxy resin. In their work, they changed the thickness direction by modifying a fused filament fabrication (FFF) 3D printer thereby proving an increase in strength of the specimens. Mohammad & Chee. (2011) [8] analysed the 3D printing effects of layer thickness and binder saturation level on the mechanical properties, integrity, and dimensional accuracy. In their work on the inkjet-based 3D printing, flexural test and tensile test were carried out by following ISO 178:2001 and ISO 527:1993 standards. Nabeel & Marius (2021) [9], verified the solid and porous continuous carbon fiber-reinforced polymer composite (CCFRPC) structures manufactured by fused deposition modeling. In their work, the grid infill pattern and density levels are varied to evaluate the tensile and flexural properties.

The work has drawn many important conclusions out of which they mentioned that carbon fiber content on mechanical properties increased both tensile and flexural strength. Camargo et al. (2019) [10], adopted Fused deposition modelling to analyse the mechanical properties of polylactic acid (PLA)-graphene filament. They varied the infill and layer thickness parameters using a statistical technique central composite design (CCD). The research findings

from the work concluded that mechanical properties increase with layer thickness but varies with the infill ratio. Guanghai Shi et al. (2020), [11], analysed a 3D printed titanium-alloy aerospace bracket designed by thermo-elastic topology optimization. A triaxial tensile test is performed to verify the designed bracket. They adopted a Selective Laser Melting (SLM) technique in the work and concluded that, weight of the part is reduced, and the strength of the part increased based on their topology optimisation. Yoram Mass & Oded Amir (2017) [12] adopted a topology optimisation approach to reduce the support material while 3D printing complex designs. The main focus of the work is on reducing the overhang features by adopting structural optimisation discrete truss-based model and continuum-based model. Their work states that the magnitude of the optimal printing direction and can provide layouts that have good printability with a limited performance drop. From an exhaustive literature review conducted, it has been clear that researchers verified the strength of the part by (i) varying 3D printing parameters (ii) modified the 3D printing setup (iii) adopted topology optimisation methods and modified the design and (iv) adopted / sandwiched two materials to evaluate the mechanical properties. It is also clear that some work has been already conducted in CFRP, but there is a gap to study the effect of infill ratio and pattern on new materials. Based on the analysis, it decided to adopt material Nylon with CFRP (Onyx) and analyse its properties by varying the infill pattern and the infill ratio. It also further decided to adopt topology optimisation and analyse the strength by comparing it with the tensile and flexural tests on a standard shape with the aim to manufacture a sample industrial part.

2. Materials, machine and software

The material considered for the experimentation and simulation is 'Onyx' plastic. 'Onyx' is a Markforged exclusive material that is comprised of Nylon plastic filled with micro carbon fibres. Basically, Carbon fibre is made up of chains of carbon atoms which form thin strands or fibres [3,4]. It is used as a reinforcement material as it can increase the strength and stiffness of a part. Onyx is chosen material because of its high strength and stiffness, and most suitable for a sample industrial part. The material properties for Onyx are shown in Fig. 3(a). It is 3D printed in a Markforged Mark 2, carbon fibre composite printer (Fig. 3(b)). The supporting software for the machine is 'Eiger' and it allows the user to import CAD files to generate printable G-Code giving options to change (i) the main material and reinforcement, (ii) apply supports and (iii) adjust the build parameters.

3. Plan and Design of Experiments

First, it has been decided that the models are designed conforming to the standard dimensions for tensile and flexural test. It is verified by following the ASTM D638 standards (Type V) [13] for tensile test and ISO 178 [14] standard for flexural tests. To manufacture these specimens, a DOE has been created varying infill ratio and infill pattern (Table 1).

Based on the above plan, 18 models made of Onyx plastic with carbon fibre were printed (Fig.4). It is with the plan to use nine models for each test. i.e 9 for tensile and 9 for flexural tests.

4. Results and discussion

4.1. Tensile test

In the work, Instron Universal Testing Machine Model 3369 has been used for both the tests. Fig. 5 (a) & (b) shows the results from

the tensile tests in the form of load extension graphs. From the graph in Fig. 5(a), the following are noticed in terms of the length extension under a tensile load (with constant triangular infill pattern) (i) the specimen with an infill ratio of 85%, extended up to 5.6 mm, for a 700 N load (ii) the specimen with an infill ratio of 65%, extended up to 5.1 mm, for a 700 N load as well (iii) the specimen with an infill ratio of 45%, extended up to 4.75 mm, for a 600 N load and (iv) the specimen with an infill ratio of 25%, was found to be the weakest under tensile load extending approximately to a length 3 mm but bearing a tensile load of 900 N. The results obtained by varying the 'infill pattern' (constant 37% infill ratio, except for solid being 100%) are shown in Fig. 5 (b). The following are observed in terms of the length extension under a tensile load (i) for the triangular infill pattern, extension is recorded up to 7.3 mm for 650 N load (ii) for the solid pattern (100% infill ratio), extension is recorded up to 6.8 mm for a 650 N load (iii) for the specimen with a hexagonal pattern, extension is recorded up to 6.2 mm for a load of 625 N. In terms of weakest specimen, a gyroid shape infill pattern, recorded the second weakest, where an extension of approximately 4.8 mm is recorded under a 625 N load.

Lastly, the rectangular infill pattern specimen has the weakest tensile strength where it recorded an extension of 4.33 mm for an 800 N load. The phenomenon of recording a higher load before failure noticed with lower infill ratio and associated pattern is because of (i) at lower infill ratio, the fine thin layers will be strongly attached to each other with highest bond strength (ii) the intermolecular distance between the carbon fibre atom and the polymer will be minimal because of effect of optimum curing temperature during / after 3D printing. But this will not be the case with higher infill ratio where there is a requirement for some higher elevated curing temperature to attain a strong intermolecular bonding. Further, when values are plotted, the yield strength and the ultimate tensile strength of the material will be closer to each other, where at this point the specimen absorbs maximum energy instantly (because of intermolecular bond strength) but fails because of thickness obtained by infill ratio.

4.2. Flexural test

Fig. 6 (a) and (b) shows the results from the flexural test in the form of load-extension graphs obtained for varied infill ratio and pattern. From the graph in Fig. 6(a), the following are noticed in terms of the bending deflection under a compressive load (with constant triangular infill pattern) (i) the specimen with an infill ratio of 85%, deflected approximately 6 mm under a load of 250 N (ii) the specimen with an infill ratio of 65%, deflected approximately 5.6 mm under a load of 340 N (iii) the specimen with an infill ratio of 45%, was found to be the specimen with the second weakest flexural strength with a bending deflection of approximately 5.4 mm under a load of 300 N. (iv) the weakest infill ratio in terms of flexural strength was found to be 25% where the deflection is approximately of 4.7 mm under a load of 350 N.

Similarly, Fig. 6(b), shows the test results obtained by varying the 'infill pattern' (constant 37% infill ratio, except for solid being 100%) from which the following can be observed (i) the gyroid infill pattern provides the highest flexural strength with an extension of 5.6 mm for a 350 N load. (ii) the triangular infill pattern shows the second highest flexural strength with an extension of 5.1 mm for a load of 300 N (iii) the hexagonal infill pattern was found to have the third highest flexural strength with an extension of 4.8 mm for a load of 280 N. (iv) the rectangular infill pattern was found to be the second weakest flexural strength with an extension of 4.7 mm for a 350 N load and (v) lastly, the solid infill pattern was found to be the weakest in terms of flexural strength with an extension of 3.9 mm for a 400 N load. From the tests, it can be

Property	Test Standard	Onyx	Nylon White
Tensile Strength (MPa)	ASTM D638	36	51
Tensile Modulus (GPa)	ASTM D638	1.4	1.7
Tensile Strain at Break (%)	ASTM D638	58	150
Flexural Strength (MPa)	ASTM D790*	81	50
Flexural Modulus (GPa)	ASTM D790*	3.6	1.4
Flexural Strain at Break (%)	ASTM D790*	N/A**	N/A**
Heat Deflection Temperature (°Celsius)	ASTM D648 Method B	145	41
Density (g/cm ³)	N/A	1.2	1.1

*Measured by a method similar to ASTM D790

**Flexural Strain at Break is not available because neither material breaks before the test ends.

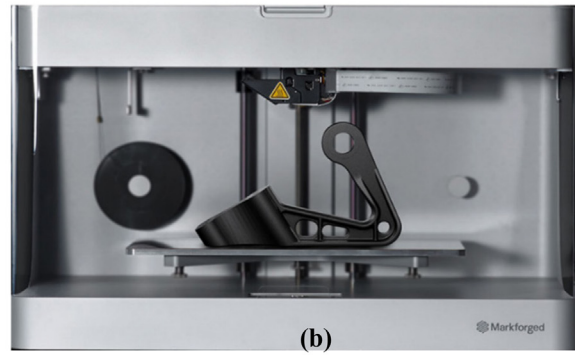


Fig. 3. (a) Material Properties of Onyx (b) Markforged Mark 2 Printer (c) Internal View of Specimen showing Carbon Fibre Distribution.

Table 1

Design of Experiment (DoE) for selected Infill Patterns and Infill Ratios for Testing.

S.No.	Infill Pattern	Infill Ratio	Mechanical Test1 (ASTM D638 (2014), Type V)	Mechanical Test2 ISO 178 (2003)
Parameter Test 1 – Varying Infill Ratio				
1	Triangular	25%	Tensile	Flexural
2	Triangular	45%	Tensile	Flexural
3	Triangular	65%	Tensile	Flexural
4	Triangular	85%	Tensile	Flexural
Parameter Test 2 – Varying Infill Pattern				
1	Triangular	37%	Tensile	Flexural
2	Gyroid	37%	Tensile	Flexural
3	Rectangular	37%	Tensile	Flexural
4	Hexagonal	37%	Tensile	Flexural
5	Solid	100%	Tensile	Flexural

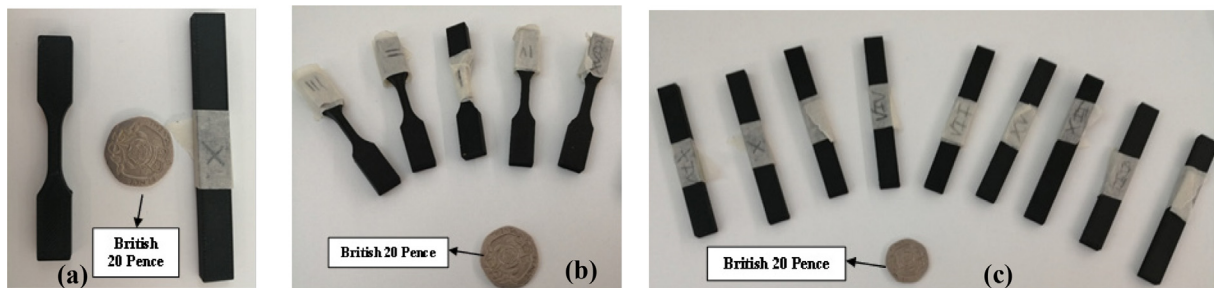


Fig. 4. (a) Tensile and Flexural Test Specimen (b) Tensile Test Specimens [13] and (c) Flexural Test Specimens [14].

noticed that the same load absorption phenomena seen in tensile testing is reflected here as well. It can also be interpreted those parts with a higher infill ratio will have a higher flexural strength. This is because as increasing the infill ratio increases the density of the part and denser materials are generally understood to have a strong stiffness. It can be deduced from these test results, that a test specimen with an infill ratio of 85% and a triangular pattern would have significantly better tensile and flexural strength.

5. Topology optimisation analysis and validation

From the above experimental testing, it has been decided to validate the findings by producing a part with optimum infill pattern and infill ratio applied to it. This was achieved by first topologically optimising an existing part (Yoram Mass & Oded Amir., (2017) p.5) considering a hypothetical load case through a static FEA analysis.

For comparison, two materials are considered (i) an Onyx material and (ii) 316L-Stainless Steel (SS). The chosen part and load case is inspired by a design challenge issued by GE (General Electric) Aviation [15] available as open-source CAD model in the 'grabcad.com' community (Fig. 7 (a)). The part is a jet engine bracket with the objective being to perform a topology optimization to reduce the mass as much as possible whilst still maintaining the strength and performance of the original. This part provides a meaningful case study for the purpose of this project as it can be used to highlight the effects of geometry within the 3D printing area. For topology optimisation ANSYS software has been adopted and a mesh convergence was used to determine the suitable mesh size and to validate the accuracy of the simulation (Fig. 7(b)). The convergence can be seen to occur from a mesh size of 25 mm at a maximum von Mises stress value of 1 MPa. Based on analysis, a suitable mesh size of 2 mm was selected, and suitable loads, suitable constraints were applied to the model. A bearing load of 50 N force

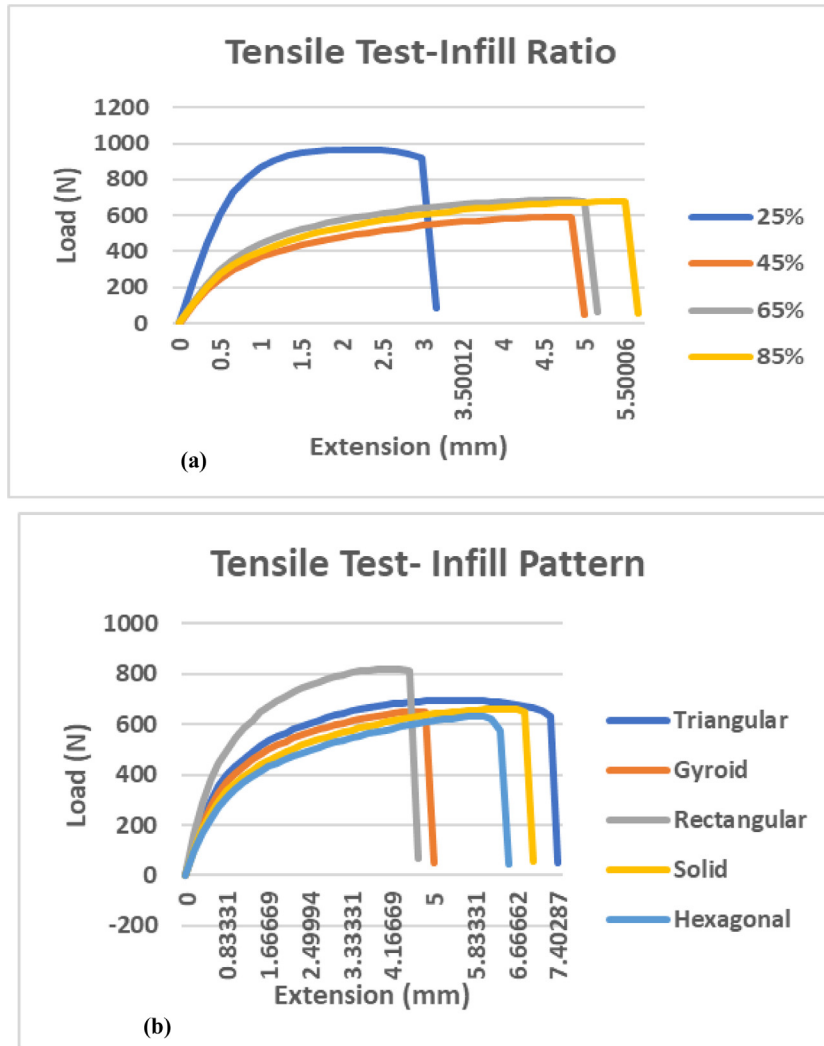


Fig. 5. Tensile Test Deflection-Load Graph for (a) Infill Ratio and (b) Infill Pattern.

is applied at 'A' (in Fig. 7(a)) and cylindrical constraints has been applied to the four supports 'B' (in Fig. 7(a)).

After meshing (Fig. 8(a)), loads are applied, and the model is simulated under the static structural simulation conditions. The results are obtained for total & directional deformation (Fig. 8(a)), maximum principal stress and strain, equivalent stress and strain. It is deduced from the analysis, that the highest deformation occurs at the area that experiences the load. The areas that are further away from this loading area experience less deformation. Owing to page restriction's only total deformation (Fig. 8(a)) has been presented here. Any further data required can be obtained from the authors. All the simulated deformations are under 0.1 mm which can be interpreted as negligible for the predicted load case. This justifies the use of optimization as the part has been arguably overengineered. Based on this, topological optimization process for the jet engine bracket is conducted. Fig. 9 (a) shows the initial optimized part geometry that was generated by the ANSYS optimization simulation. The structure is organic in appearance, so is unlikely to be manufactured in that form. Fig. 9 (b) shows the geometry after it has been cleaned and smoothed in the ANSYS Space Claim software. This model is more manufacturable than the first optimized model however it still has an organic and irregular appearance. A redesigned model inspired

by the optimized model is shown in Fig. 9 (c). This new model has been utilized and the same outputs were measured against the original FEA simulation discussed earlier in this section.

Fig. 10 (a) & (b) shows the deformation contour plots for the optimised bracket considering the Onyx and 316L-SS. It is noticed that the results are more comparable to the original bracket made of onyx compared to the onyx optimised bracket. The deformation is again low enough and not be a concern for the function of the part. Table 2 is presented with the comparative summary of results from the analysis for the optimised bracket model considering Onyx and 316L-SS. It can be seen that the steel model performs better than the onyx model in terms of deformation and strain. However, the steel part does experience a higher amount of stress than the onyx part does. Neither of the parts fail, this means that, for the studied load case, either of the parts would be suitable for use. As onyx has a lower density and is cheaper, both in terms of manufacturing and material, it is reasonable to recommend that it would be preferable to use the onyx. If the part was deemed to be critical and required a higher factor of safety, then the steel bracket may be preferable. This again further investigation considering the application required in an industrial scenario. The final redesigned part has been 3D printed part with the optimum parameter values and is presented Fig. 11 (a) & (b).

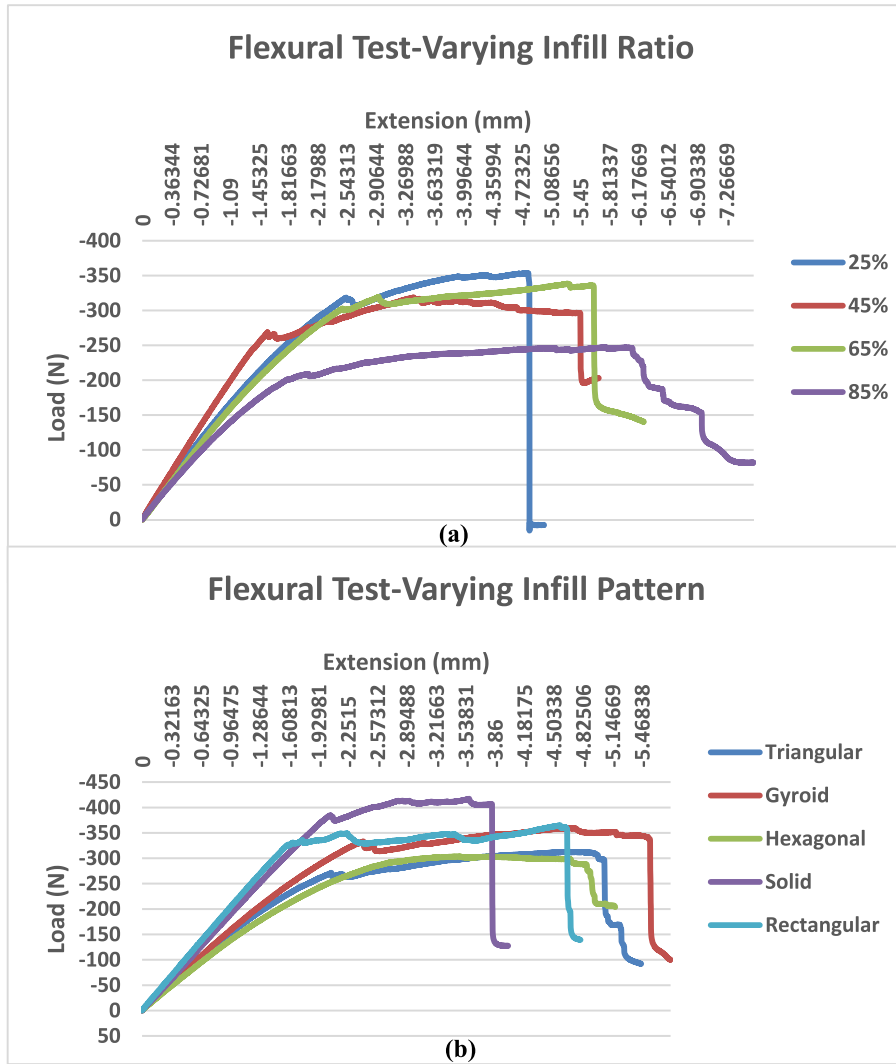


Fig. 6. Flexural Test Deflection-Load Graph for (a) Infill Ratio and (b) Infill Pattern.

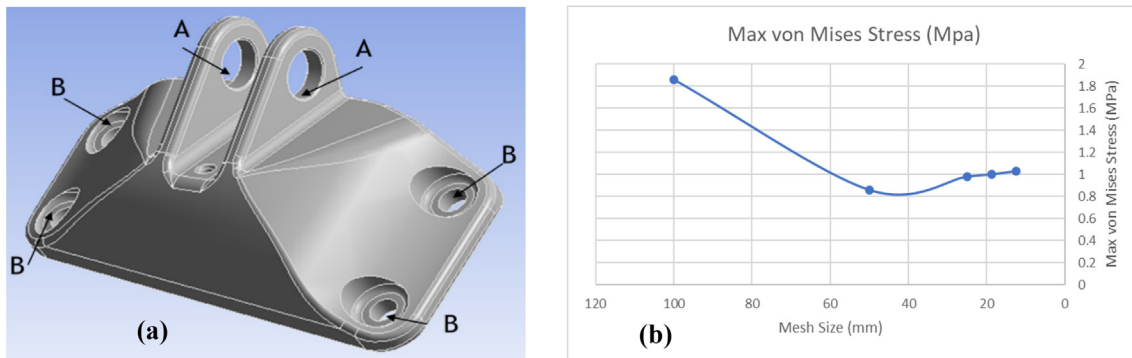


Fig. 7. (a) CAD model - Design challenge issued by GE (General Electric) Aviation (Carter et.al (2014) p.2.) (b) Mesh Convergence Study.

6. Conclusions

In this work, Onyx material (nylon) is 3D printed by reinforcing carbon fibres to conduct a fundamental study varying two process parameters namely infill ratio and infill pattern. This is with the aim to analyse the tensile and flexural strengths and their suitability on industrial parts. The results revealed some interesting corre-

lation between the material usage (infill ratio) and internal structural design (infill pattern). It is obvious that higher amount of material usage will give higher flexural and tensile strength. The same was true with our tensile test specimen with 85% infill ratio with constant triangular infill pattern, where it recorded a highest length extension of 5.6 mm for a load of 700 N. The lowest being 25%, with a length extension of 3 mm for a load capacity of

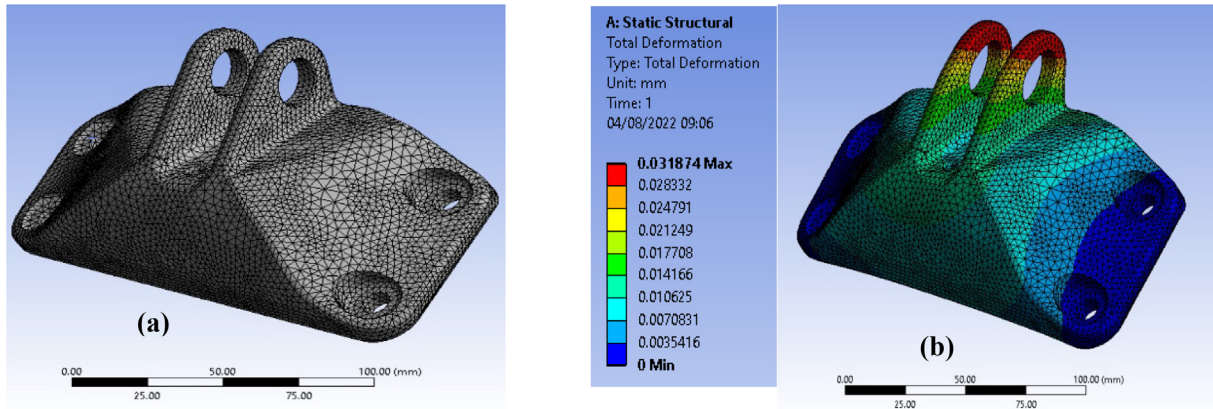


Fig. 8. (a) Meshed model with 2 mm element size (a) Original Bracket Model Total Deformation Contour Plot.

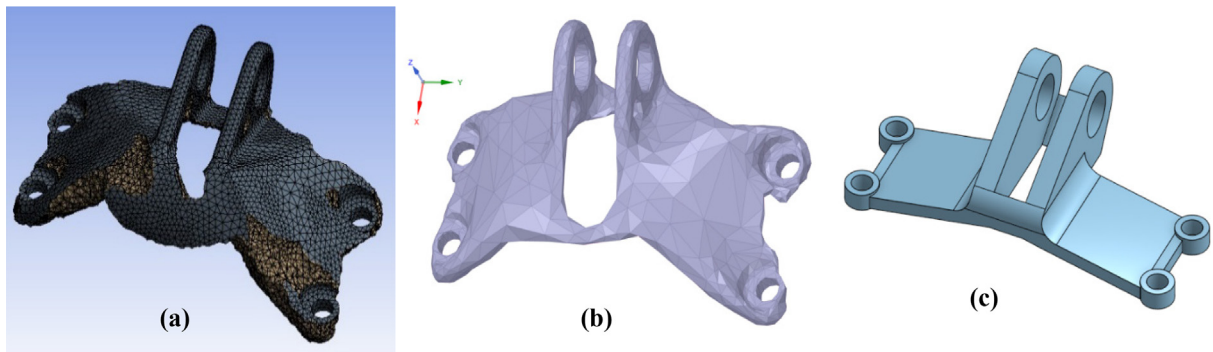


Fig. 9. (a) Generated Optimised Bracket Model; (b) Smoothed Optimised Bracket Model; (c) Re-designed CAD Model for Manufacture.

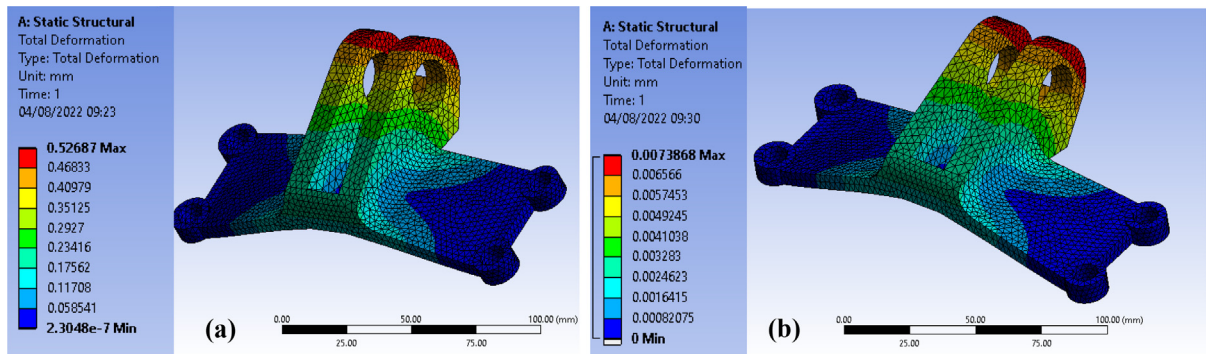


Fig. 10. Total Deformation Contour Plot for redesigned model (a) Onyx (b) 316L-SS.

900 N. But in terms of infill pattern it was different, where with constant infill ratio of 37%, triangular shape pattern recorded a

Table 2
FEA Analysis Comparison between Onyx and Steel Grade 316L-SS optimised models.

Properties	Onyx	316L-SS
Total Deformation (mm)	0.530.	0.01
X-axis Deformation (mm)	0.04	5.50E-04
Y-axis Deformation (mm)	0.36	0.01
Z-axis Deformation (mm)	0.16	0.02
Equivalent Von Mises Strain	0.002	2.63E-05
Maximum Principal Strain	0.002	2.55E-05
Minimum Principal Strain	1.23E-06	2.20E-08
Equivalent Von Mises Stress (MPa)	3.08	4.78
Maximum Principal Stress (MPa)	2.93	5.14
Minimum Principal Stress (MPa)	0.28	0.31

highest length extension of 7.3 mm under a 650 N. When compared to the solid pattern where the infill ratio is set to 100%, the length extended approximately to 6.8 mm under a 650 N load. The results prove how optimal structural design change can reduce the overall material usage and leads to sustainable manufacturing. The lowest extension of 4.33 mm is recorded for an 800 N load d the rectangular infill pattern specimen. This lower infill ratio and simpler pattern absorbing higher load before failure led to one more interesting conclusion where strong bonding at lower levels of infill ratio can be noticed owing to proper temperature during curing. More in-depth investigation is required for this case and is planned for the scope of future work. Similar results are noticed in case of flexural tests where 85% infill ratio recorded a bending deflection of approximately 6 mm under a compressive load of 250 N, and gyroid infill pattern providing a highest flexural

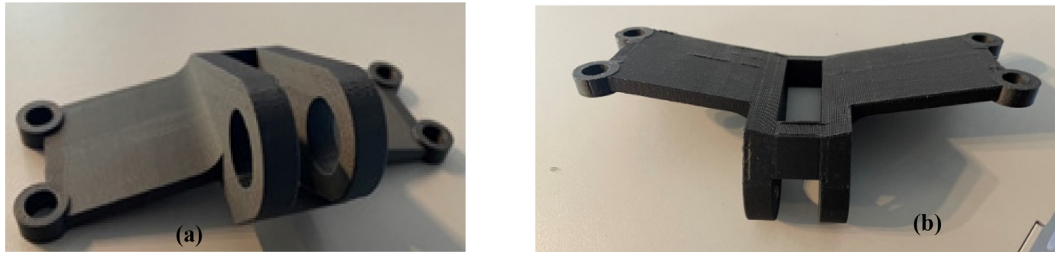


Fig. 11. 3D printed Optimised Jet Engine Bracket (a) Top View (b) Bottom View.

strength with an approximate extension of 5.6 mm for a 350 N load. It can be deduced from the test results, that a test specimen with an infill ratio of 85% and a triangular pattern would have significantly better tensile and flexural strength. Based on these values a real-time part has been selected and simulated in ANSYS under static loading conditions. This is then topologically optimised and verified for design suitability. A new model is redesigned and again a static simulation is conducted considering two materials (i) Onyx and (ii) 316L-SS. Once the simulation is completed the values are compared with each other and with the original part. The results were agreeable and by using the optimal values of process parameters a final model is 3D printed. A further comparative study is planned for this component with another real time industrial product.

Data availability

Data will be made available on request.

Declaration of Competing Interest

The authors declare the following financial interests/personal relationships which may be considered as potential competing interests: Arivazhagan Anbalagan reports administrative support was provided by Coventry University. Arivazhagan Anbalagan reports a relationship with Coventry University that includes: employment.

Acknowledgements

Authors would like to sincerely thank Wendy Garner, Head of School, Coventry University, UK, for supporting this research under school funding. The authors also like to extend their sincere thanks to Dr. Phil Green, Steven Allitt, Coventry University, UK for supporting 3D printing and Testing.

References

- [1] S.H. Masood. Advances in Fused Deposition Modeling. *Comprehensive Materials Processing* 2014; Elsevier, 10, 69-91
- [2] M.d. Hazrat Ali, Z. Smagulov, T. Otepbergenov, Finite element analysis of the CFRP-based 3D printed ankle-foot orthosis, *Procedia Comput. Sci.* 179 (2021) 55–62.
- [3] M.Manoj Prabhakar, A.K. Saravanan, A.Haiter Lenin, I.Jerleno, K.Mayandi, P. Sethu Ramalingam. A short review on 3D printing methods, process parameters and materials. *Materials Today Proceedings* 2021; 45, 6108–6114
- [4] Ting Wang, Nanya Li, Guido Link, John Jelonnek, Jürgen Fleischer, Jorg Dittus, Daniel Kupzik. Load-dependent path planning method for 3D printing of continuous fiber reinforced plastics. *Composites: Part A* 2021; 140, 106181.
- [5] N. Kumekawa, Y. Mori, H. Tanaka, R. Matsuzaki, Experimental evaluation of variable thickness 3D printing of continuous carbon fiber-reinforced composites, *Compos. Struct.* 288 (2022).
- [6] Keiichi Shirasu, Masayoshi Mizutani, Naoki Takano, Hajime Yoshinaga, Tsuyoshi Oguri, Ken-ichi Ogawa, Tomonaga Okabe, Shigeru Obayashi. Lap-shear strength and fracture behavior of CFRP/3D-printed titanium alloy adhesive joint prepared by hot-press-aided co-bonding. *International Journal of Adhesion & Adhesives* 2022; 117, 103169.
- [7] J. Kajimoto, J. Koyanagi, Y. Maruyama, H. Kajita, R. Matsuzaki, Automated interlaminar reinforcement with thickness directional fiber arrangement for 3D printing, *Compos. Struct.* 286 (2022).
- [8] M. Vaezi, C.K. Chua, Effects of layer thickness and binder saturation level parameters on 3D printing process, *Int. J. Adv. Manuf. Technol.* 53 (2011) 275–284.
- [9] N. Maqsood, M. Rimasauskas, Tensile and flexural response of 3D printed solid and porous CCFRPC structures and fracture interface study using image processing technique, *J. Mater. Res. Technol.* 14 (2021) 731–742.
- [10] J.C. Camargo, A.R. Machado, E.C. Almeida, E.F.M.S. Silva, Mechanical properties of PLA-graphene filament for FDM 3D printing, *Int. J. Adv. Manuf. Technol.* 103 (2019) 2423–2443.
- [11] G. Shi, C. Guan, D. Quan, W.u. Dongtao, L. Tang, T. Gao, An aerospace bracket designed by thermo-elastic topology optimization and manufactured by additive manufacturing, *Chin. J. Aeronaut.* 33 (4) (2020) 1252–1259.
- [12] Y. Mass, O. Amir, Topology optimization for additive manufacturing: accounting for overhang limitations using a virtual skeleton, *Addit. Manuf.* 18 (2017) 58–73.
- [13] ASTM D638. *Standard Test Method for Tensile Properties of Plastics* 2014.
- [14] ISO 178. *International Standard, Plastics - Determination of Flexural properties.* 2003.
- [15] T.W Carter, D.J. Erno, D.H.Abbott, C.E Bruck, G.H. Wilson, J.B.Wolfe, D.M. Finkhousen, A.Tepper, R.G.Stevens. *The GE Aircraft Engine Bracket Challenge: An Experiment in Crowdsourcing for Mechanical Design Concepts* 2014.